applied sciences

MDPI

Article

Study on Sedimentary Evolution of the Hanjiang River Delta during the Late Quaternary

Yang Wang [1], Liang Zhou [2], Xiaoming Wan [1], Xiujuan Liu [2,*], Wanhu Wang [1,*] and Jiaji Yi [1]

[1] Haikou Marine Geological Survey Center, China Geological Survey, Haikou 570100, China
[2] Hubei Key Laboratory of Marine Geological Resources, China University of Geosciences, Wuhan 430074, China; zhouliang2812@stu.ouc.edu.cn
* Correspondence: xjliu@cug.edu.cn (X.L.); wangwanhu@mail.cgs.gov.cn (W.W.)

Abstract: In recent years, coastal areas have been threatened by many potential hazards due to global warming, glacier melting and sea level rise. Understanding their evolutionary history and development trends can help predict disasters and further reduce the corresponding losses. The Hanjiang River delta in the southeastern part of China is the second largest delta in Guangdong Province and has such challenges. Studying the sedimentary evolution and delta initiation of the Hanjiang Delta is beneficial for understanding the response of the Hanjiang Delta to present and future sea level and climate changes. In this research, we drilled a series of cores from the Hanjiang subaqueous delta, which contains information on the sedimentary environment, climate change and sea level change during the late Quaternary. Combined with previous research results and under the constraint of high-precision and high-resolution AMS^{14}C and OSL, we carried out a multi-proxy analysis that included micropaleontology and grain size to obtain information on the sedimentary environment, sea level change and climate change. We then further discussed the initiation of the Hanjiang delta and its primary factors. The Quaternary sediments began depositing in the early Late Pleistocene (MIS5), and three sedimentary cycles can be recognized from bottom to top. The dating results also indicate that the first two cycles were formed during the late Pleistocene, while the last cycle was formed during the Holocene. The initiation of the Hanjiang Delta was indicated by a progradation in the process of a transition from estuary to a typical delta. At this time, the rate of delta progradation seaward was fast, and increasing amounts of sediments moved through the third line of islands into the sea. The barrier–lagoon system began to develop in the estuary of Hanjiang during this period. With the sequential construction of the delta, the lagoon was filled and covered by delta deposition, and the barrier bar moved to the sea; thus, the barrier-coast delta depositional model was established in the study area. Since the last glacial period (LGM), the Hanjiang River Delta and other river deltas in the region seem to have experienced similar evolutionary histories, including the filling of incised paleo-valleys and estuaries in the Early Holocene and deltaic progradation in the Middle to Late Holocene, controlled by sea level change.

Keywords: Hanjiang River Delta; late Quaternary; estuary; deposition

Citation: Wang, Y.; Zhou, L.; Wan, X.; Liu, X.; Wang, W.; Yi, J. Study on Sedimentary Evolution of the Hanjiang River Delta during the Late Quaternary. *Appl. Sci.* **2023**, *13*, 4579. https://doi.org/10.3390/app13074579

Academic Editor: Oleg S. Pokrovsky

Received: 1 February 2023
Revised: 30 March 2023
Accepted: 31 March 2023
Published: 4 April 2023

1. Introduction

Estuarine deltas connect rivers and oceans and collect abundant geological information on land–sea interactions [1,2]; these areas promote the progress and development of human society [3]. However, in recent years, coastal erosion, ground deposition and inundation of coastal lowlands caused by global warming and sea level rise may have affected the sustainable economic development of the estuary delta. The increased potential for natural disasters in estuary delta areas means that we must understand their sedimentary evolution history to develop and utilize them more reasonably.

In the past few decades, the late Quaternary sedimentary evolution and initial delta construction of large river deltas in East Asia and Southeast Asia, including the Yellow

River, Yangtze River, Pearl River, Red River and Mekong River, have been comprehensively studied. However, the small- and medium-sized river deltas in this area have received less attention. The Hanjiang River Delta is a typical representative of the medium-sized river delta in East Asia. Therefore, an analysis of the late Quaternary sedimentary evolution process of the Hanjiang River Delta can provide representative geological information as a reference for the study of late Quaternary sedimentary records, sea level and climate change in small- and medium-sized estuary deltas and their adjacent continental shelf areas.

The study of deltas can be traced back to the end of the 19th century. Galloway (1975) divided the world's major river deltas into three categories: the Mississippi River Delta, which represents river-dominated deltas; the San Francisco River delta in Brazil and the Senegal River Delta in Africa, which represent wave-dominated deltas; and the Ganges Delta and the Basheng-Langa River Delta in Malaysia, which represent tidal-dominated deltas [4]. Since the middle and late 20th century, the concepts of chronology and sequence stratigraphy have been widely used and developed in geology. With the deepening of human research on Earth system science, the stratigraphic structure and sedimentary evolution of postglacial river deltas have become the focus attention of scholars [1]. The latest research suggests that global climate and sea level changes have a certain unity, though regional characteristics can be found [5].

The main factors affecting the evolutionary history of river deltas are sea level changes, monsoon climate and human activities in the late Quaternary [6], which makes the river delta region an excellent place to judge human activities, climate change and sea level changes. Although current research exhibits substantial differences and uncertainties, it has still received extensive attention from scholars inside and outside of China [7–9]. Since the late Quaternary river delta system has certain similarities with the evolution process of the present and future delta regions, to reduce these uncertainties, we need to better understand the evolution process of modern delta regions.

There are different views on the vertical variation in Quaternary sedimentary facies in the Hanjiang Delta. Zhang [10] believed that the Quaternary deposits in the western Shantou-Raoping fault zone can be divided into three parts: the lower part is continental sand and gravel with clay, the middle part is marine clay and sand layer, and the upper part is continental and artificial fine and medium sand accumulation. The Quaternary to the east of the fault zone is also divided into three parts, but the lower and upper parts are marine strata and the middle is continental strata; some sections under the lower marine strata have more than ten meters of continental deposits [10]. For the Hanjiang River Delta, Chen (1984) established five major sedimentary cycles according to the vertical variation in the grain size of the Quaternary sediments. Each cycle shows a sedimentary rhythm of coarse (gravel, sand) and fine (silt, clay) sediments [11].

There are currently four viewpoints on the age of the Hanjiang River Delta: Early Pleistocene, Middle Pleistocene, Early Late Pleistocene and Holocene. There is considerable controversy among these viewpoints [9–11]. We believe that the accuracy of dating needs to be further discussed due to the limitations of current dating techniques. In addition, the drilling data based on previous studies are mostly distributed in the plain area of the Hanjiang River Delta, and there is a relative lack of research on the sea area.

In this research, we used geological drilling information to establish the stratigraphic structure of the sea area outside the Hanjiang Estuary. To define the stratigraphic age before the Holocene and the postglacial delta construction time, the characteristics of late Quaternary sedimentary evolution in the sea area outside the Hanjiang Estuary were analyzed by means of: sediment lithology division; AMS ^{14}C and optically stimulated luminescence dating; foraminiferal and ostracod identification; particle size testing; and clay mineral content determination. According to the analysis of strata and sedimentary environment, the period and age of late Quaternary transgression were analyzed, and the paleoenvironment and paleoclimate changes were speculated. These results were combined with the results of previous calculations of regional relative sea level height for

a discussion on the characteristics of regional sea level change. Based on accurate dating data and sedimentary facies analysis results, the sedimentary evolution characteristics of the Hanjiang Delta since the late Quaternary are discussed. Importantly, the OSL age of the underlying marine strata of ZK03 borehole also confirms the high sea level phenomenon in the study area during MIS5. In addition, the rich information of sedimentary environment changes in the Hanjiang River Delta revealed in this study, such as sea level changes, can provide the possibility for extracting historical environmental change information. It also provides support for delta land use and future development planning of coastal zone.

2. Materials and Methods

2.1. Geological Context of the Study Area

The Hanjiang River Delta is located below Chaozhou City in northeastern Guangdong Province, China. It is the second largest delta in the coastal area of South China after the Pearl River Delta. The magmatic rocks in the Hanjiang delta area are mainly Yanshanian intrusive rocks and Himalayan magmatic rocks. Yanshanian intrusive rocks are the most widely distributed rocks in the Hanjiang Delta. These rocks intruded into the upper Jurassic volcanic rock series, placing their formation age in the late Jurassic or its later period; hence, they are the products of late Yanshanian magmatic activity. It is generally believed that the Hanjiang Delta accepted Quaternary sediments in the middle and late Pleistocene. According to the absolute age, sedimentary facies and sedimentary cycle analysis, sporopollen climate analysis and sea level change analysis of the Quaternary sediments in the Hanjiang River Delta, Li (1987) divided the Quaternary strata of the Hanjiang River Delta into groups. These groups are the Nanshe Formation in the lower part of the middle section of the upper Pleistocene, Jiali Formation in the upper part of the middle section of the upper Pleistocene, Tuopu Formation in the upper section of the upper Pleistocene, Lianxia Formation in the lower Holocene, Chaozhou Formation in the lower section of the middle Holocene, Chenghai Formation in the upper section of the middle Holocene and Dongli Formation in the upper Holocene [12]. In addition, the Hanjiang delta is located on the southeast side of the second compound uplift belt of the Neocathaysian structure [10]. The Hanjiang River Basin is characterized by hilly areas, and the Hanjiang River is a typical mountainous medium and small river.

2.2. Research Material

From June to August 2020, based on previous papers, monographs and geological survey reports, the Haikou Marine Geological Survey Center of China Geological Survey constructed 9 geological boreholes (ZK01-03, HK01-06) in the sea area outside the Hanjiang River estuary, Guang'ao Bay, Haimen Bay and other areas (Figure 1). The average core rate of core sediment was >95%. After the geological logging of the cores of 9 boreholes was completed, the different lithology strata were divided. A total of more than 600 sediment samples were collected from different lithology strata. Each sediment sample was tested for grain size, and some horizon samples in ZK03, ZK01, HK01 and HK03 were selected to carry out age tests and micropaleontological analyses.

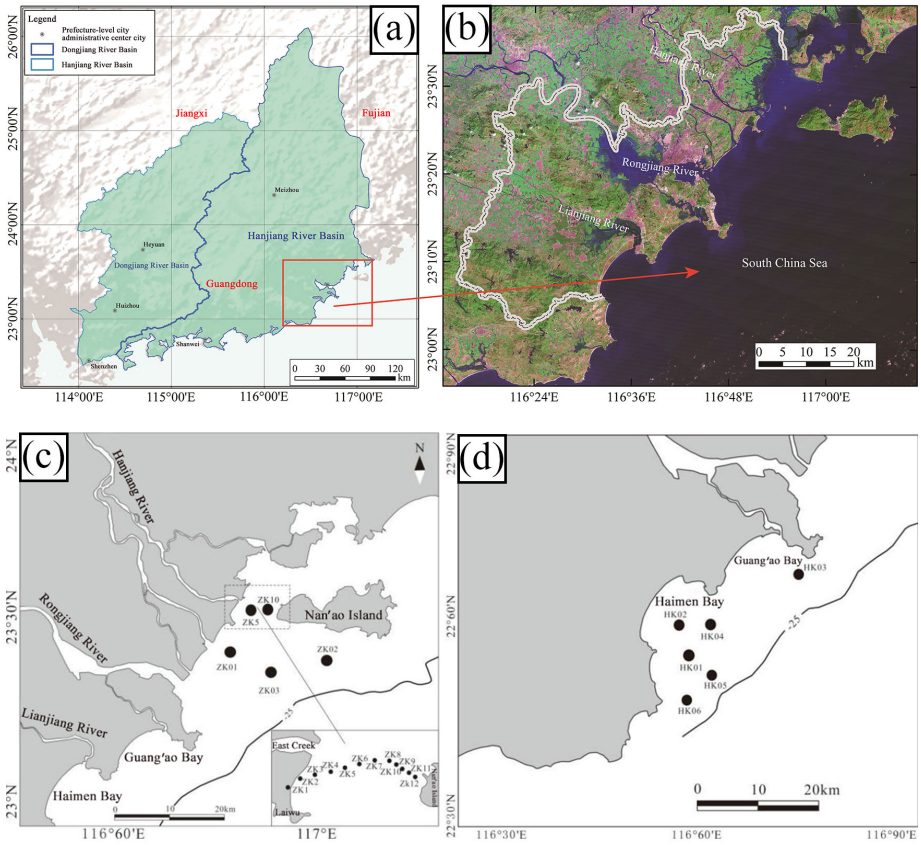

Figure 1. Borehole distribution map of the study area: (**a**) Location map of the study area; (**b**) Remote sensing image of the study area; (**c**) The sea area outside Hanjiang Estuary; (**d**) Haimen Bay and Guang 'ao Bay.

2.3. Experimental Method

2.3.1. Age Determination

1. AMS ^{14}C

The AMS ^{14}C radioactive age is very important to the study of the Quaternary sedimentary evolution of the Hanjiang River Delta. The effective selection of test materials determines the accuracy of the test results. Gastropod shells, plant debris and peat in sediments are effective dating materials. We sent the samples of 8 layers of the ZK03, HK01 and HK03 holes to the State Key Laboratory of Marine Environmental Science of Xiamen University for AMS ^{14}C. The experimental results show that there are 3 foraminifera samples and 5 carbonaceous mud sediment samples. We used the CALIB 5.0 program to correct the AMS ^{14}C radioactive age data of the test results to the calendar age. The marine13 correction curve was selected for marine inorganic carbon samples such as shells. Since the samples were from the coastal zone where the sea and land interact, the organic matter in the silt samples was selected from the mixing curve of the ocean and the Northern Hemisphere atmosphere. According to the research of Southon et al. about the effect of regional marine carbon reservoirs in the South China Sea, we used $\Delta R = -25 \pm 20$ an in the correction process.

2. OSL age

The main dating materials are quartz and feldspar in silt and sandy samples. Under shading conditions, we vertically inserted a black cylindrical sample container (approximately 2 cm in diameter) into the core and immediately covered the sample after sampling to avoid direct exposure to the sun. We sampled eight layers in the ZK03, ZK01, HK01, ZK02 and HK05 boreholes and completed the test work in the State Key Laboratory of Offshore Marine Environmental Science of Xiamen University. The apparatus was a Day-

break 2200, the excitation light source was blue light (488 ± 15 nm) and infrared light (880 ± 60 nm), the signal was detected with a PMT QA9235 photomultiplier tube, and the intensity of the irradiation source was 0.055 Gy/Sec.

2.3.2. Microfossil Analysis

A total of 50 samples were collected from ZK03, HK01, HK03, HK06 and other boreholes. The fossils of foraminifera and ostracods were processed and analyzed, and the biostratigraphic age was divided according to the fossil assemblage and paleoenvironment. The micropaleontological assemblages of these samples were analyzed, and they were sent to the Micropaleontological Laboratory of the School of Earth Sciences, China University of Geosciences (Wuhan) for the preparation and analysis of microfossils. Sample handling complied with the National Standard of the People's Republic of China (GB/T 12763.8–200)—Microfossil analysis procedures in marine survey specifications.

The micropaleontological analysis included six steps: sample drying, 10% H_2O_2 soaking dispersion, standard mesh sieve washing, identification statistics, sample under the microscope and sample slag drying (Figure 2).

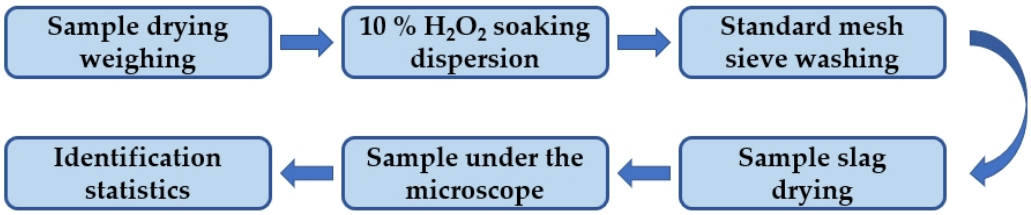

Figure 2. Analysis and processing flow of micropaleontological fossil samples.

The foraminiferal fossil samples were selected under a Nikon SMZ1000 stereomicroscope, and the relative abundance of common species and exinite types (percentage in the total number of samples) and the simple differentiation of species in the samples (number of fossil species contained in each sample) were counted and calculated. If there were too many samples, the reduction method was employed; usually, the number of samples was greater than 300.

2.3.3. Grain Size Test

Grain size is an important structural feature of sediments and the basis for their classification and naming. It is usually used for sedimentary research, sedimentary environment research, material movement, hydrodynamic conditions and particle size trend analysis. The particle size of the sediment should be analyzed by a particle size analyzer. There are three kinds of particle size analyzers: nanometer particle size analyzers, laser particle size analyzers and single particle light resistance particle size analyzers. The laser particle size analyzer used in this study is from the Geological Survey Experimental Center, Institute of Geological Survey, China University of Geosciences, Wuhan. The instrument model is a Mastersizer-3000 laser particle size analyzer produced by the British Malvern Company.

The test process includes two steps: sample pretreatment and on-machine testing. Sample pretreatment removes calcareous components and organic matter and fully utilizes technology to increase the accuracy and reliability of the results. During the last pretreatment, each sample was tested three times. After completion, the test data were checked, and those with poor repeatability were measured again.

The surface sediments are named by the Folk classification of marine sediments. The Udden–Wentworth grade scale, the limit of Wentworth grade and its classification were used to determine the grain size of the borehole sediments. The average grain size (Mz), sorting coefficient (σ), skewness (SK) and kurtosis (KG) were calculated by the Fokker and Ward diagram.

3. Results

3.1. Strata Age

The AMS ^{14}C and OSL dating results show that the deeper the strata are, the older the strata (Tables 1 and 2). The OSL dating data of two sediments at the bottom of the ZK03 borehole showed a reversal phenomenon, which may be due to the pollution of the samples during the sampling process. The age of the Holocene sediments in the upper part of the borehole is approximately 10 ka BP, the age of the lower part of the last glacial river environment or exposed weathered sediments is roughly between 17–30 ka BP, and the oldest strata at the bottom of the Quaternary sediments in the study area is ~90 ka BP.

Table 1. AMS^{14}C results obtained for borehole samples.

Borehole Number	Depth/m	Dating Materials	Average Calendar Age/ka BP	Error/ka
ZK03	34.5	mud	24.1	±0.18
ZK03	37.5	mud	27.9	±0.26
ZK03	39.7	mud	37.4	±0.70
HK01	2	foraminiferan	2.4	±0.03
HK01	8.5	mud	8.1	±0.05
HK01	24.3	mud	30.2	±0.31
HK03	3	foraminiferan	3.2	±0.04
HK03	5.2	foraminiferan	5.0	±0.04

Table 2. OSL results obtained for borehole samples.

Borehole Number	Depth/m	Dating Materials	Age/ka BP	Error/ka
ZK03	40.9	Grey medium fine sand	55.8	±5.8
ZK03	64.7	Dark gray argillaceous fine sand	96.7	±13
ZK03	74.1	Bluish gray muddy silty sand	74.2	±8.2
ZK01	38.0	Grayish yellow medium sand	52.6	±7.5
HK01	26.1	Dark gray medium sand	17.3	±2.3
HK01	33.1	Dark gray sandy clay	55.9	±6.1
ZK02	21.8	Dark gray medium fine sand	67.2	±5.3
HK05	13.5	Grayish yellow sandy clay	16.2	±1.9

3.2. Abundance of Foraminifera and Ostracods

Benthic foraminifers and ostracods are mainly divided into nearshore species (living in estuaries and nearby tidal flats with salinitie of 1–31), inland shelf species (living in continental shelf waters below 50 m with salinitie of 20–31) and euryhaline species (living in open waters above 50 m with salinitie >31). Microscopically, foraminifera fossils were found in a small number of layers in each borehole. Some layers had more foraminifera than others. The abundance of ostracods was low, and they were better preserved. The abundance of fossil species is shown in Tables 3 and 4.

A total of 22 samples were collected from borehole ZK03. We found 18 species of benthic foraminifera, of which 13 were calcareous transparent shells, 5 were porcelain shell types, and no cemented shell type was found. These species were mainly located in the middle of the formation (17 m, 25–29 m, 34.5 m). The dominant species of foraminiferal fauna in the borehole were Asterorotalia subtrispinosa and Ammonia, which had the highest abundance in the 25–27 m layer, with an average of 100/50 g dry sample. This fauna is a typical coastal shallow water assemblage dominated by warm water and contains a certain salty sea–land transitional facies.

Table 3. ZK03, HK03, HK01 and HK06 Statistics of Foraminiferal Abundance in Part of Borehole.

Sample Number	Depth/(m)	Number of Shell Statistics	Bonded Shell		Porcelain Shell														Calcium Transparent Shell															
			Textularia sp.	*Textularia foliacea*	*Spiroloculina* sp.	*Quinqueloculina laevigata*	*Quinqueloculina seminula*	*Quinqueloculina lamarckiana*	*Quinqueloculina akneriana*	*Quniqueloculina* sp.	*Massilina laevigata*	*Triloculina tricarinata*	*Flintina bradyana*	*Guttulina* sp.	*Glandulina* sp.	*Cibicides* sp.	*Hanzawaia nipponica*	*Hanzawaia convex*	*Rotalidium annectens*	*Rotalinoides compressiusculus*	*Ammonia beccarii* var.	*Ammonia* spp.	*Ammonia tepida*	*Asterorotalia substrispinosa*	*Asterorotalia diplocava*	*Asterorotalia binhaiensis*	*Eponides* sp.	*Rosalina bradyi*	*Pararotalia inermis*	*Pseudorotalia schroeteriana*	*Cribrononion subincertum*	*Elphidium advenum*	*Elphidium hispidulum*	*Elphidium* sp.	*Elphidium crispum*	*Nonion commune*	*Nonion* sp.
ZK03	17	25	0	0	0	2	0	0	0	2	0	0	0	0	0	0	0	0	0	0	4	5	0	4	0	0	0	0	1	0	0	2	0	4	0	1	0
ZK03	25	385	0	0	0	2	0	2	2	5	1	0	0	0	0	0	0	0	2	0	6	11	2	321	3	5	0	0	2	0	1	7	0	9	0	2	2
ZK03	27	115	0	0	0	0	0	0	0	1	0	0	0	0	0	0	0	0	0	0	5	18	0	78	2	2	0	0	2	0	0	2	0	5	0	0	0
ZK03	29	33	0	0	0	0	0	0	0	0	0	0	0	0	0	0	0	0	0	0	11	14	0	1	0	0	0	0	0	0	0	3	0	4	0	0	0
ZK03	34.5	48	0	0	0	0	0	0	0	0	0	0	0	0	0	0	0	0	0	0	0	3	0	36	0	2	0	0	0	1	0	3	0	2	1	0	0
HK03	3	101	0	0	1	2	0	11	1	24	5	0	0	0	0	0	0	0	1	0	0	0	0	0	0	0	4	0	16	18	0	7	2	6	3	0	0
HK03	5.2	355	1	1	6	13	2	62	11	47	32	3	2	1	0	2	0	2	64	4	7	6	0	0	0	0	8	0	12	0	0	22	5	12	5	16	11
HK01	2	411	0	0	2	12	2	33	5	14	4	2	0	0	2	3	3	0	188	1	2	4	0	0	0	0	0	1	0	0	0	14	5	9	1	92	12
HK01	4	280	0	0	2	13	1	31	9	17	1	4	2	0	0	4	2	0	63	2	3	5	1	0	0	0	0	1	0	0	0	25	26	17	4	36	11
HK06	10.3	9	0	0	0	0	0	0	0	0	0	0	0	0	0	0	0	0	0	1	1	1	0	1	0	0	0	0	0	0	0	3	0	2	0	0	0

Table 4. Statistics of ostracod abundance in some layers of ZK03, HK03, HK01 and HK06 holes.

Drilling Number	Depth/m	*Sinocytheridea longa*	*Sinocytheridea impressa*	*Albileberis sinensis*	*Albileberis* sp.	*Sinocytheridea* sp.	*Pontocythere minuta*	*Stigmatocythere costa*	*Stigmatocythere roesmanisis*	*Bicornucythere bisanensis*	*Neonomoceratina delicata*	*Neomonoceratina chenae*	*Keijella kloempritensis*	*Keijella bisanensis*	*Neocytheretta faceta*	*Pistocythereis* sp.	*Pistocythereis subovata*
ZK03	17	0	0	1	0	0	0	0	0	0	0	0	0	0	0	0	0
ZK03	25	3	1	0	0	1	1	0	0	3	2	2	1	0	0	0	0
ZK03	27	0	0	0	0	0	0	0	0	2	0	0	0	0	0	0	0
ZK03	29	0	0	0	0	0	0	0	0	1	0	0	0	0	0	0	0
ZK03	34.5	17	22	8	2	1	0	0	2	4	3	4	3	2	2	4	2
HK03	3	3	1	0	0	0	1	0	0	2	0	1	0	0	0	0	0
HK03	5.2	47	8	1	3	4	0	1	1	6	4	7	2	3	2	1	2
HK01	2	17	15	8	16	14	3	3	5	21	13	14	13	18	15	9	17
HK01	4	14	6	2	4	4	0	0	0	5	7	4	5	2	4	6	16
HK06	10.3	1	2	2	0	0	0	0	0	0	1	1	0	0	0	0	0

Nine samples were detected in core HK03, and 23 kinds of benthic foraminifera were found in the upper strata (3 m, 5.2 m), 16 of which were calcareous transparent shells and 6 of which were porcelain shells; cemented shells accounted for only 1 genus and 2 species, with an overall abundance of general, an average of 115/50 g dry sample. The dominant species of the foraminiferal fauna in the borehole was Rotalidium annectens, which accounted for 40–50% of the whole group, followed by the porcelain shell type, mainly represented by Quinqueloculina lamarckiana, which accounted for more than 10%. In addition, there were many porcelain shells that were severely worn, and the first-level classification of species could not be seen. High levels of *Pseudorotalia schroeteriana*, a typical macrobenthic foraminifera of the warm-water shallow-water type, were found in calcareous transparent shells. The species composition of the fauna was a typical nearshore shallow water combination dominated by warm water molecules. The degree of shell preservation was poor, with a broken shell rate of approximately 40%.

Seventeen samples were detected in core HK01, and 22 benthic foraminiferal species appeared in the uppermost layer (2 m to 4 m), including 14 calcareous transparent shell types and 8 porcelain shell types; the overall abundance was medium, with an average of 456/50 g dry sample, and the shells were preserved in medium to good conditions. The dominant species of the foraminiferal fauna found in this borehole was *Rotalidium annectens*, accounting for approximately 50–60% of all faunas, and Nonion commune, accounting for approximately 12% of all faunas. Quinqueloculina lamarckiana represented approximately 8% of the total fauna. The species composition of the fauna was dominated by typical warm-water nearshore shallow water assemblages, namely, Rotalidium annectens-Nonion commune.

Two samples were detected in core HK06, and foraminifera appeared only at the bottom of the horizon (10.6 m). Only 6 species of calcareous transparent shells of the benthic type were found, for a total of 9 shells, which were *Rotalinoides Compressiuscula*, *Ammonia beccarii* var., *Ammonia* spp., *Asterorotalia subtrispinosa*, *Elphidium advenum* and *Elphidium* sp. The genera and species of foraminifera found in this layer were relatively simple, and the individuals were small, consisting primarily of common molecules in the nearshore transitional facies combination.

Ostracod fossils were found in only 10 layers of the tested samples, and the differentiation degree was low. The surface ornamentation of most of the selected ostracod shells was clear, and the boreholes and layers where ostracod individuals appeared intensively were ZK03-17 m, ZK03-25 m, ZK03-27 m, ZK03-29 m and ZK03-34.5 m, for a total of 94 individuals; HK03-3 m, HK03-5.2 m, for a total of 100; HK01-2 m, HK01-4 m, for a total of 280; and hK06-10.3 m, for a total of 7. A total of 21 species of 9 genera were identified by the stereomicroscopy observation and photography. *Sinocytheridea longa*, *Albileberis sinensis*, *Albileberis* sp., *Sinocytheridea* sp., *Bicornucythere bisanensis*, *Neomonoceratina chenae*, *Keijella kloempritensis* and *Keijella bisanensis* were the most abundant genera in the whole sampling borehole. The majority of the fauna are common in coastal areas of China, with some genera and species, such as *Stigmatocythere*, seen not only in modern coastal areas of China and the Quaternary but also in the Pliocene–Modern deposits of Indonesia. Additionally, *Bicornucythere bisanensis* is the most common eurythermal species in the marginal seas of the western Pacific and has been reported in Japan, Indonesia and Malaysia [13].

3.3. Particle Size Analysis

The average particle size reflects the average kinetic energy condition of medium transport. The average particle size of the ZK03 sediment is 1.77–173.5 μm (Figure 3), and the particle size changes greatly, indicating that the hydrodynamic conditions in the study area since the late Quaternary have experienced a shock, causing an alternating sedimentary environment. The grain size of the borehole sediments is generally coarse, and the content of the particles above the silt grain size is more than 60%. In the layers of more than 8 m, 18–40 m and 60–70 m, the mud content increases, exceeding 20%, which reflects strong sedimentary hydrodynamic conditions. In the 0–40 m and below-60 m layers, the

contents of clay and silt are relatively high. In addition, the sorting coefficient reflects the dispersion and concentration of sediment particles, and a smaller value indicates better sorting. The overall sorting coefficient of the ZK03 sediment is 0.584–3.544, indicating poor sorting. Vertically, the standard deviation of the 0–20 m horizon is 0.6–2.3, indicating poor sorting. The remaining horizon standard deviations are generally 2.0–3.5, indicating poor sorting. Each layer of the whole borehole shows a large fluctuation, reflecting the poor sediment sorting caused by unstable hydrodynamic conditions. Skewness is used to represent the symmetry of the frequency curve, reflecting the proportion of coarse and fine particles in the sediment. The skewness of most samples in the ZK03 borehole is positive or nearly symmetrical, and the range of variation is large. The 0–30 m, 60–66 m and 70–75.8 m layers have positive skewness, and the particle size distribution is biased toward fine-grained components, while only the 30–38 m, 40–45 m, 54–60 m and 66–70 m parts of the sample have a slightly negative deviation, biased toward the coarse-grain end. The peak state is used to illustrate the sharpness or bluntness of the curve compared with the normal frequency curve and reflects the concentration of the particle size distribution. The smaller the value is, the higher the sharpness. The peak state of the ZK03 borehole is mostly above 0.9, which is nearly normal or sharp, indicating that the later sedimentary environment causes less modification to the sediment; thus, the original sedimentary environment of the sediment is represented.

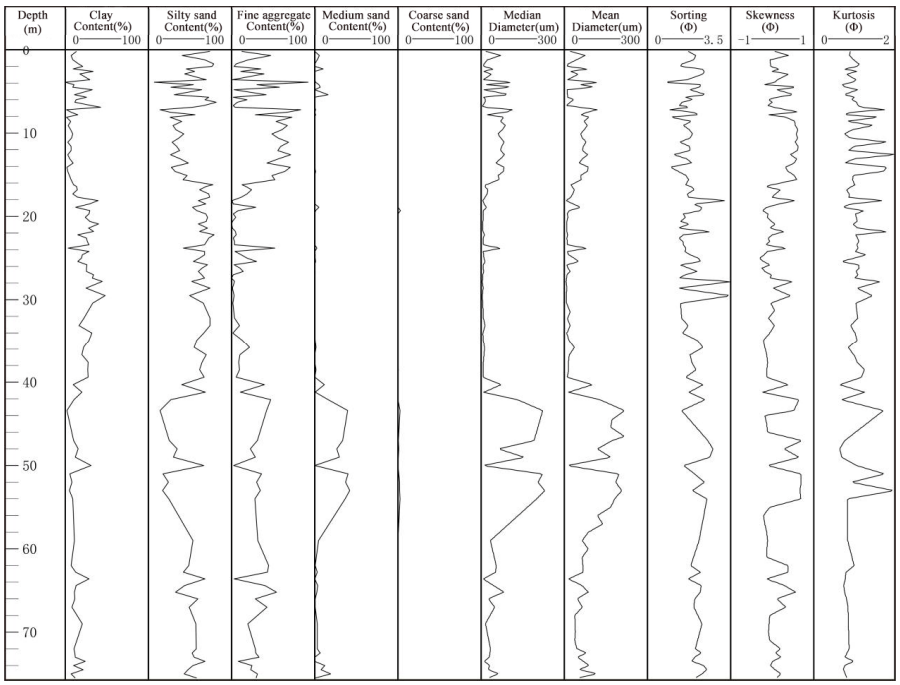

Figure 3. Grain size parameter variation of ZK03 borehole sediment.

Similarly, the content of each component of the ZK01 borehole 0–2 m changes little, and the average particle size is small, indicating that the hydrodynamic conditions are weak. The contents of fine sand and clay at 2–4 m changes greatly, indicating that the hydrodynamic force experienced a large change at that time. The sorting is 2.0–3.0, indicating very poor sorting. The sample areas of 4–34 m from bottom to top are mainly silt and clay, and the average particle size gradually decreases and finally stabilizes, indicating that the hydrodynamic force gradually weakens, and sorting and skewness also reflect this change. The clay content at 34–38 m gradually decreases from top to bottom, mostly less than 20%, while the clay content below 35 m is less than 10%. The content of medium sand and fine sand changes greatly, the sorting is mostly 2–3, and the fluctuation is large, indicating that the hydrodynamic conditions in this period are strong, and the fluctuation is violent and unstable. The average particle size of 38–42 m is small, with positive skewness,

and the particle size distribution is biased toward fine-grained components. The average content of 42–50 m clay is less than 10%, the average content of sand is more than 60%, and the sorting coefficient changes greatly, indicating that the hydrodynamic fluctuation is strong, the skewness is negative, and the coarse grain is biased. The 50–52.4 m component is mostly composed of clay and silt. The sand content gradually decreases, and the average particle size decreases to below 50 μm, indicating that the hydrodynamic force is medium (Figure 4).

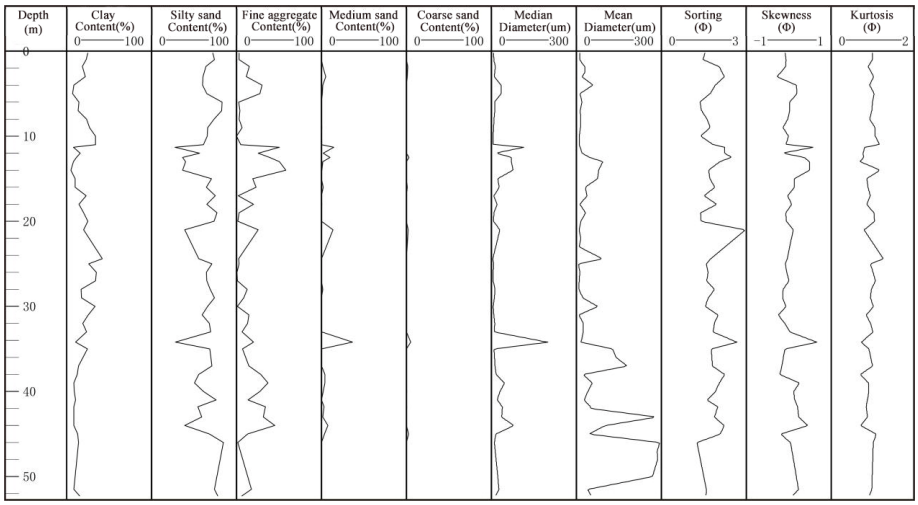

Figure 4. Grain size parameter variation diagram of ZK01 borehole sediment.

On the Pasuge C-M images, Zone 1 generally reflects strongly hydrodynamic riverbed deposition, with mass movement dominated by displacement. Area 2 reflects tidal channel deposition with strong hydrodynamics, which is dominated by saltation and displacement. Zone 3 reflects the sediments of the estuary sandbar, beach and sandbank with medium hydrodynamic strength, which is dominated by saltation. Zone 4 reflects the weak natural levees, crevasse splay, tidal flats and other deposits, which are mainly suspension and displacement ones. Areas 5 and 6 reflect the weak hydrodynamic delta front and front slope, delta plain, flood plain, stagnant water depression and other deposits, which are mainly suspension ones. In the borehole core, the hydrodynamic conditions reflected by the sediment transport mode indicate the sedimentary environment and sedimentary cycle.

The sediment sample points of ZK030–3.9 m mainly fall in the C-M image 6 area, are mainly suspended sediment, and the hydrodynamic force is weak. The 9–4.5 m sediment sample points mainly fall in C-M image area 3, are mainly for saltation deposition, and the hydrodynamic force is strong, which may represent a short regression after river sedimentation; the 4.5–30.4 m sediment sample points mainly fall in C-M image areas 5 and 6, are mainly for sediment transport, and the hydrodynamics force is weak. The 30.4–32.2 m sediment sample points mainly fall in C-M image area 3, are mainly for saltation deposition, and the hydrodynamic force is strong. The 32.2–42.1 m sediment sample points mainly fall in C-M image area 6, being mainly suspended sediment, and the hydrodynamic force is weak; the 42.1–54 m sediment sample points mainly fall in C-M image area 3, being mainly for saltation deposition, and the hydrodynamic force is strong; the 54–75.5 m sediment sample points mainly fall in C-M images 5 and 6, being mainly suspended sediment, and the hydrodynamic force is weak (Figure 5).

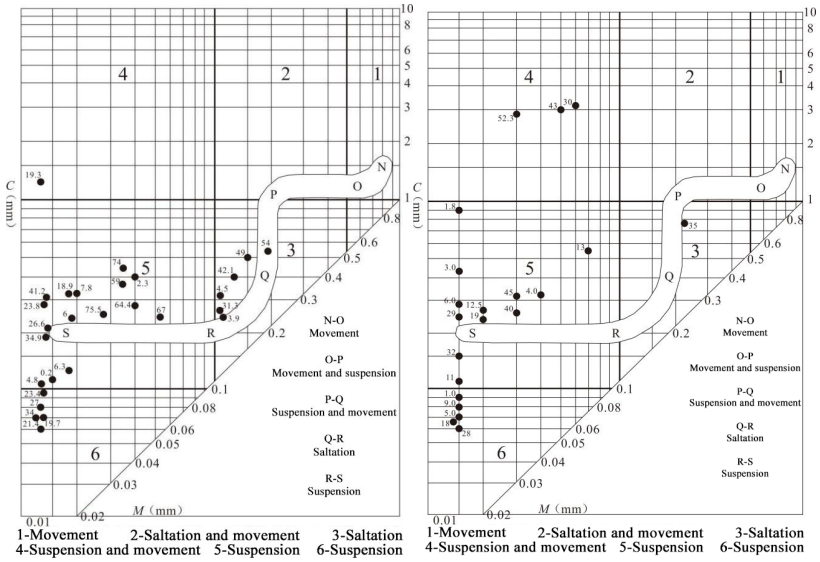

Figure 5. Grain size falling point map of Passeig C-M image of ZK03/ZK01 borehole sediments.

Similarly, the 0–30 m sediment sample points of the ZK01 borehole mainly fall in the 5th and 6th areas of the C-M image, being mainly suspended sediment, and the hydrodynamic force is weak. The 30–37 m sediment sample points mainly fall in C-M image area 3, are mainly for saltation deposition, and the hydrodynamic force is strong; the 37–43 m sediment sample points mainly fall in the C-M image 6 area, are mainly suspended sediment, and the hydrodynamic force is weak. The 43–52.3 m sediment sample points mainly fall in the C-M image 4 area, are mainly suspended load and bed load deposition, and the hydrodynamic force is medium (Figure 5).

4. Discussion

4.1. Age of Earliest Acceptance of Quaternary Sediments: MIS 3 or MIS 5

The most controversial issues in coastal sediment dating concern the MIS3 and MIS5 stages. In principle, the maximum limit for analytical measurements with the AMS radiocarbon dating method is approximately 60 ka. In this study, AMS ^{14}C and OSL dating methods were combined to constrain the earliest sedimentary age of the Quaternary in the Hanjiang Delta in the MIS5 period; the study included lithology, grain size analysis, dating and foraminifer abundance statistics of ZK03 sediments outside the Hanjiang River estuary. Grain size analysis reveals the transition process from marine fine-grained clay ~ silt to coarse sandy sediments, which can better reflect the characteristics of the transition from MIS5 high sea level to MIS4 low sea level. Predecessors believe that the Quaternary sediments in the Hanjiang River Delta began in the middle of the late Pleistocene. On the one hand, because only AMS 14C is used, it is impossible to accurately measure the age of strata greater than 60 ka; on the other hand, the drillings at that time were mainly distributed in the Han River Delta land area. Due to the tectonic background of the overall subsidence of the Han River Delta in the late Quaternary and the obstruction of the third island mounds, the terrain of the Han River Delta area during MIS5 was much higher than the current elevation of the sedimentary basement of the marine strata, and the transgression may not have reached the Han River Delta plain area.

4.2. Sedimentary Evolution Process

The results of OSL dating at the bottom of the ZK03 drilling hole show that the oldest Quaternary stratum in the Hanjiang Delta was in the MIS5 period. The grain size, clastic minerals and paleontological characteristics of sediments show that this section is a flood plain–floodplain deposit. During 90–70 ka BP, the global sea level was in a relatively high sea level period [13]. The strata in the study area during this period were alternately formed

by massive sand and mud, composed of mildly layered hard mud and silty sediments, and contained peat fragments, but no shells or marine indicators were found. It is speculated that this section is an estuarine–beach sedimentary environment. During this period, the study area experienced a change in the sedimentary environment from continental facies to marine facies. Due to the barrier of the third island mound, the influence range of this transgression was small, and no record of this transgression was found inside the delta plain.

At approximately 70 ka BP, the Earth entered the last glacial period [13], the seawater withdrew from the delta plain, and a set of medium coarse sand-weathered clay layers was deposited. The global sea level was relatively low during the last glacial period, but there was still a period of relatively high sea level. The second transgression in the study area occurred after the late Pleistocene, and sedimentary strata with silty clay and muddy fine sand as the main sedimentary types were developed, representing the shallow marine sedimentary environment defined by the interactions between river and seawater tidal dynamics. At approximately 30 ka BP, this transgression reached its high sea level period [14–16]. Then, until the arrival of the last glacial maximum (26–17 ka BP), the sea level dropped to its lowest level [12–14], and a set of continental bottom gravel layers developed in the study area. Some boreholes also found porphyritic weathered clay and yellow–white clay sandy gravel layers.

The Hanjiang River Delta began to accept postglacial deposition at approximately 10.4 ka BP, and the sea level began to rise rapidly, reaching the maximum transgression range at approximately 6.3 ka BP, during which time the sedimentary characteristics changed many times. The sedimentary evolution process of the study area since the Holocene can be divided into three stages from the old to new in chronological order. At approximately 10.4–8.5 ka BP, the end of the last glacial period, the global climate began to gradually become warm and humid, and at approximately 9.2 ka BP, after gradually transforming into marine deposits, the estuary environment developed. At approximately 8.5–6.3 ka BP, the composition of foraminiferal species represented a typical coastal shallow water combination, mainly warm water molecules, and contained a certain proportion of euryhaline transitional phase molecules, representing the coastal–shallow sea estuary sedimentary environment. At approximately 6.3–0 ka BP, large-scale regression led to the continuous diffusion of sediments carried by rivers to the open sea, and the strong wave action in the open sea led to the redistribution of sediments from the basin into the open sea. The sediments were distributed along both sides of the estuary and parallel to the coastline, forming a series of barrier sand dams. After the maximum transgression, the study area began to construct the Holocene delta and gradually formed the current land–sea pattern. In addition, dredging has had a certain impact on the deposition of coastal waters. Since we visited and investigated, no dredging has occurred in the coastal waters of the study area. Only the channel in the Rongjiang Estuary has been dredged on a small scale, which has little effect on the sedimentary evolution of the whole study area.

4.3. Holocene Delta Formation and Barrier–Lagoon System

After the Hanjiang Delta region reached the Holocene maximum transgression at approximately 6.3 ka BP [17], the sea began to retreat. Under the dynamic marine background of weak tidal action and strong wave action in the bay, coupled with the blocking effect of the third row of island mounds in the bay, the river action in the outer sea area is relatively weak. Strong offshore waves distribute and redistribute the sediments along both sides of the estuary, forming a series of barrier bars. As the delta advances to the sea, sediment gradually accumulates outside the third island mound to form a coastal sand bank, which is a coastal sandy sedimentary body composed of a large number of intertidal organisms, shells and coarse-grained sediments. Due to the barrier between the coastal sandbanks and the third island mound, the sea water in the inner edge is prevented from entering the open sea. Tidal action causes this sea water to enter the inner edge of the third island mound along the intermittent sandbanks. This situation, coupled with the low-lying terrain in the

western region, leads to tidal influx, forming the lagoon inside the third island mound. The Holocene barrier–lagoon system developed in this area, and then the sedimentary evolution of the barrier coastal delta began. In the late Holocene, the change in the sea level began to stabilize. As the delta continued to advance to the sea, the barrier–lagoon system also continued to move to the sea.

From the last glacial period to the early Holocene, the sea level began to rise rapidly, and the early Holocene transgression led it to reach the maximum range [18–20]. At this time, the main sedimentary environment of the Hanjiang Delta was mainly shore–shallow sea and shallow bay. The low-density flow of the Hanjiang River into the sea was a plane jet, which led to a relatively stable water environment after the sediments of the Hanjiang River entered the estuary. A large number of river sediments began to be deposited there, and with hydrodynamic action, they spread to the open sea, forming the main body of the delta plain dominated by river action [21]. At this time, the barrier coastal delta was in the formation period, the main sediment lithology was the continental margin alluvial plain channel sand body and the underwater front sand body, and the fine-grained sediments diffused to the open sea via marine dynamic action (Figure 6).

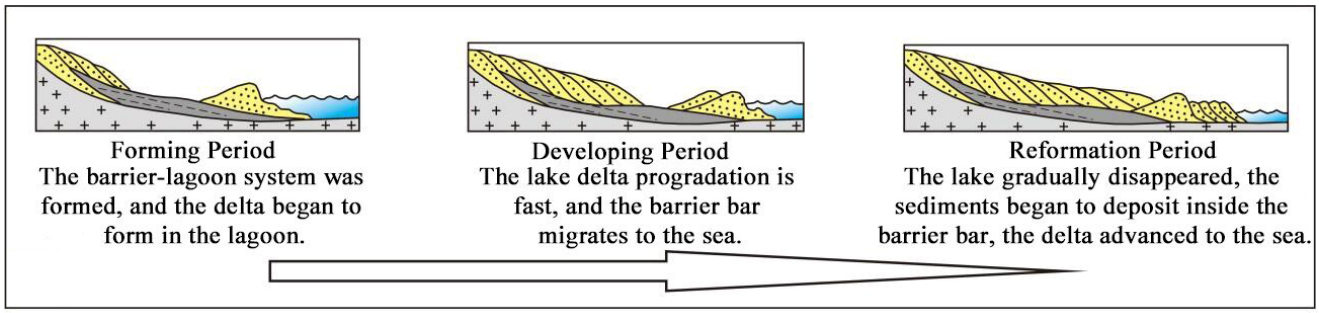

Figure 6. Evolution stage of barrier coastal delta.

After the maximum transgression, the delta began to advance to the sea, and a large amount of sediment was transported out to the sea through the third island mound. The barrier–lagoon system began to develop, inhibiting the outward diffusion of river sediments and accelerating delta construction. In the eastern part of the lagoon, due to the shallow water body, a large number of river sediments were deposited, and delta construction advanced rapidly. Delta deposits dominated by river action were developed. On the west side of the lagoon, due to the relatively low-lying terrain, the tidal water influx deepened the water body in the area, and the lagoon swamp sedimentary environment became completely different from that in the eastern region. Inside the lagoon, a certain scale of fan-shaped delta plain deposits dominated by river sand developed. Outside the barrier, a large amount of sediment accumulates under the action of oceanic dynamics, forming a large number of sandbars that were distributed parallel to the coastline and advanced toward the sea (Figure 6).

In the late Holocene, the sea level tended to be stable and equal to the present sea level. The Hanjiang River Delta advanced to the open sea beyond the barrier, and the strong wave action hindered the delta from advancing to the sea; this delta still exists inside the lagoon delta plain. At this time, the delta had been pushed out of the third island hills, and the sediments in the basin continued to accumulate due to wave action, forming a new barrier sand bar parallel to the coastline (Figure 6) and gradually evolving into the current barrier coast of the Hanjiang Delta.

5. Conclusions

Through the lithology description of the ZK03, ZK01 and HK01 borehole sediments in the Hanjiang River Delta and the identification of micropaleontological fossils and particle size tests, combined with previous research results and under the constraints of high-resolution and high-precision AMS^{14} C and OSL age framework, the late Quaternary

sedimentary evolution process of the Hanjiang River Delta was discussed. The main research results are as follows:

(1) The study area began to accept Quaternary sediments in the early Late Pleistocene (MIS5). A total of 10 sedimentary units developed from the bottom to the top of the Late Quaternary sediments, which mainly experienced a floodplain environment and estuary–beach environment in the early Late Pleistocene; a floodplain environment, coastal shallow sea environment, bar–lagoon environment, coastal shallow sea environment, and floodplain environment in the middle and late Pleistocene; and an estuary environment, bar–lagoon environment and delta sedimentary environment in the Holocene. From bottom to top, the study area is mainly divided into three sedimentary cycles. Each sedimentary cycle shows a sedimentary rhythm from coarse to fine from bottom to top, starting with medium and coarse sand or gravel deposition and ending with muddy silt or clay deposition. The first and second cycles belong to the late Pleistocene, and the third cycle belongs to the Holocene.

(2) After the maximum transgression in the Holocene, the progradation rate of the Hanjiang River Delta was fast, and increasing amounts of sediments converged to the sea through the third row of island mounds. Under the dynamic marine background of weak tidal action and strong wave action in the bay, coupled with the blocking effect of the third island mound in the bay, the sediments imported into the open sea were redistributed along both sides of the estuary and parallel to the coastline, forming a series of barrier–lagoon systems. With the continuous construction of the delta, the lagoon water body was filled with delta deposits, and the barrier bar moved to the sea. In this cycle, the study area developed a unique barrier–lagoon coastal delta deposit.

Author Contributions: Data curation, Y.W.; formal analysis, Y.W. and L.Z.; funding acquisition, Y.W. and X.W.; investigation, J.Y. and W.W.; methodology, L.Z.; project administration, X.L. and X.W.; writing—original draft, Y.W.; writing—review and editing, Y.W., X.L. and X.W.; visualization, W.W. and J.Y.; supervision, X.L. All authors have read and agreed to the published version of the manuscript.

Funding: Comprehensive Geological Survey of Chaoshan Coastal Zone, grant number DD20208013; Comprehensive Survey of Natural Resources in Huizhou-Shanwei Coastal Zone, grant number DD20230415.

Acknowledgments: Chaoshan Coastal Zone, grant number DD20208013; Huizhou-Shanwei Coastal Zone, grant number DD20230415.

Conflicts of Interest: The authors declare no conflict of interest. The funders had no role in the design of the study; in the collection, analyses, or interpretation of data; in the writing of the manuscript; or in the decision to publish the results.

References

1. Stanley, D.J.; Warne, A.G. Worldwide initiation of Holocene marinedeltas by Decelera-tion of sea-level rise. *Science* **1994**, *265*, 228–231. [CrossRef] [PubMed]
2. Maloney, J.M.; Bentley, S.J.; Xu, K.; Obelcz, J.; Georgiou, I.Y.; Miner, M.D. Mississippi River subaqueous delta is entering a stage of retrogradation. *Mar. Geol.* **2018**, *400*, 12–23. [CrossRef]
3. Sun, Z.; Li, G.; Yin, Y. The Yangtze River deposition in southern Yellow Sea during Marine Oxygen Isotope Stage 3 and its implications for sea-level changes. *Quat. Res.* **2015**, *83*, 204–215. [CrossRef]
4. Galloway, W.E. Process framework for describing the morphologic and stratigraphic evolution of deltaic depositional systems. *Houst. Geol. Soc.* **1975**, 87–98.
5. Bard, E.; Hamelin, B.; Arnold, M.; Montaggioni, L.; Cabioch, G.; Faure, G.; Rougerie, F. Deglacial sea-level record from Tahiti corals and the timing of global meltwater discharge. *Nature* **1996**, *382*, 241–244. [CrossRef]
6. Fan, D.; Wu, Y.; Zhang, Y.; Burr, G.; Huo, M.; Li, J. South Flank of the Yangtze Delta: Past, present, and future. *Mar. Geol.* **2017**, *392*, 78–93. [CrossRef]
7. Zhang, Q.; Liu, C.; Zhu, C. Impact of environmental changes on human activities during the holocene in the Changjiang (Yangtze) river delta region. *Mar. Geol. Quat. Geol.* **2004**, *24*, 9–15.

8. Wang, Z.; Saito, Y.; Zhan, Q.; Nian, X.; Pan, D.; Wang, L.; Chen, T.; Xie, J.; Li, X.; Jiang, X. Three-dimensional evolution of the Yangtze River mouth, China during the Holocene: Impacts of sea level, climate and human activity. *Earth-Sci. Rev.* **2018**, *185*, 938–955. [CrossRef]
9. Han, M.K.; Wu, L.; Liu, Y.F.; Mimura, N. Impacts of sea-level rise and human activities on the evolution of the pearl River Delta, South China. *Proc. Mar. Sci.* **2000**, *2*, 237–246.
10. Zhang, H. Faulting and the Formation and Development of Hanjiang Delta. *Acta Oceanol. Sin.* **1983**, *5*, 202–211.
11. Chen, G. Preliminary understanding of the Holocene transgression and regression in the Hanjiang and Rongjiang rever deltas. *Mar. Sci. Bull.* **1984**, *3*, 39–44.
12. Li, P.R.; Huang, Z.G.; Zong, Y.Q. *Hanjiang Delta*; China Ocean Press: Beijing, China, 1987.
13. Sun, J.-l.; Xu, H.L.; Wu, P.; Wu, Y.-B.; Qiu, X.-L.; Zhan, W.-H. Late Quaternary sedimentological characteristics and sedimentary environment evolution in sea area between Na'ao and Chenghai, eastern Guangdong. *J. Trop. Oceanogr.* **2007**, *26*, 30–36.
14. Cao, Q. *Characteristics of Palaeoceanographical and Palaeoenvironmental Evolution since the Pleistocene in the Okinawa Trough*; The Institute of Oceanology, Chinese Academy of Sciences: Beijing, China, 2002.
15. Lea, D.W.; Martin, P.A.; Pak, D.K.; Spero, H.J. Reconstructing a 350 ky History of Sea Level Using Planktonic Mg/Ca and Oxygen Isotope Records from a Cocos Ridge Core. *Quat. Sci. Rev.* **2002**, *21*, 283–293. [CrossRef]
16. Fairbridge, R.W. Eustatic changes in sea level. *Phys. Chem. Earth* **1961**, *4*, 99–185. [CrossRef]
17. Siddall, M.; Rohling, E.J.; Almogi-Labin, A.; Hemleben, C.; Meischner, D.; Schmelzer, I.; Smeed, D.A. Sea-level fluctuations during the last glacial cycle. *Nature* **2003**, *423*, 853–858. [CrossRef] [PubMed]
18. Zhao, B.; Wang, Z.; Chen, J.; Chen, Z. Marine sediment records and relative sea level change during Late Pleistocene in the Changjiang delta area and adjacent continental shelf. *Quat. Int.* **2008**, *186*, 164–172. [CrossRef]
19. Zong, Y.Q. Postglacial Stratigraphy and Sea-Level Changes in the Han River Delta, China. *J. Coast. Res.* **1992**, *8*, 1–28.
20. Nguyen, V.L.; Ta, T.; Saito, Y. Early Holocene initiation of the Mekong River delta, Vietnam, and the response to Holocene sea-level changes detected from DT1 core analyses. *Sediment. Geol.* **2010**, *230*, 146–155. [CrossRef]
21. Hori, K.; Saito, Y. An early Holocene sea-level jump and delta initiation. *Geophys. Res. Lett.* **2007**, *34*, L18401. [CrossRef]